

ORIGINAL ARTICLE

Altered olivocerebellar activity patterns in the connexin36 knockout mouse

SARAH P. MARSHALL¹, RUBEN S. VAN DER GIESSEN², CHRIS I. DE ZEEUW² & ERIC J. LANG¹

¹Department of Physiology & Neuroscience, New York University, School of Medicine, New York, USA, and ²Department of Neuroscience, Erasmus MC, Rotterdam, The Netherlands

Abstract

The inferior olive (IO) has among the highest densities of neuronal gap junctions in the nervous system. These gap junctions are proposed to be the underlying mechanism for generating synchronous Purkinje cell complex spike (CS) activity. Gap junctions between neurons are formed mostly by connexin36 proteins. Thus, the connexin36 knockout (Cx36KO) mouse provides an opportunity to test whether gap junction coupling between IO neurons is the basis of CS synchrony. Multiple electrode recordings of crus 2 CSs were obtained from wildtype (Wt) and Cx36KO mice. Wts showed statistically significant levels of CS synchrony, with the same spatial distribution as has been reported for other species: high CS synchrony levels occurred mostly among Purkinje cells within the same parasagittally-oriented cortical strip. In contrast, in Cx36KOs, synchrony was at chance levels and had no preferential spatial orientation, supporting the gap junction hypothesis. CS firing rates for Cx36KOs were significantly lower than for Wts, suggesting that electrical coupling is an important determinant of IO excitability. Rhythmic CS activity was present in both Wt and Cx36KOs, suggesting that individual IO cells can act as intrinsic oscillators. In addition, the climbing fiber reflex was absent in the Cx36KOs, validating its use as a tool for assessing electrical coupling of IO neurons. Zebrin II staining and anterograde tracing showed that cerebellar cortical organization and the topography of the olivocerebellar projection are normal in the Cx36KO. Thus, the differences in CS activity between Wts and Cx36KOs likely reflect the loss of electrical coupling of IO cells.

Key words: *Oscillation, synchrony, connexion, multielectrode, cerebellum*

Introduction

Gap junctions are the physical substrate for electrical synaptic transmission (1). One of the first areas in the mammalian CNS where neuronal gap junctions and electrical coupling of neurons was demonstrated was the inferior olive (IO) (2,3). These initial findings led to the hypotheses that gap junctions between IO neurons served to underlie synchronous activity in the olivocerebellar system, and that such activity was critical to the role of this system in motor coordination. Consistent with these hypotheses, synchronized olivocerebellar activity has been observed both in the IO itself (4,5) and in the cerebellar cortex, as synchronous Purkinje cell complex spike (CS) activity (6–8), and patterns of synchronous CS activity have been associated with movements (9,10).

Evidence consistent with the gap junction hypothesis of synchronous CS activity has also been obtained. IO neurons were demonstrated to be

electrically coupled, both *in vivo* and *in vitro*, and to display synchronized subthreshold oscillations (3,4,11). Furthermore, the synchronization and regularity of these oscillations are sensitive to the level of gap junction coupling of IO neurons (5,12). However, whether such synchronous subthreshold oscillatory activity is the basis of CS synchrony remains to be established. In fact, there are arguments why it may not. For example, after cerebellar nuclear lesions, CS activity is highly synchronous but non-rhythmic (at least no evidence of any rhythmicity is present in autocorrelograms) (13). Pharmacological studies also provide indirect support for the gap junction hypothesis. Synchronous CS activity remains following block of both excitatory (glutamatergic) and inhibitory (GABAergic) synaptic transmission within the IO (13–15), and disappears following the injection of carbenoxolone, a non-specific gap junction blocker, into the IO (16). While these results are strong evidence in favor of the gap junction hypothesis, they are not necessarily

definitive. For example, carbenoxolone is not highly specific, as it blocks glial as well as neuronal gap junctions, and can affect other ionic membrane conductances.

Because of these questions, here we used a different approach to test this hypothesis: multiple electrode recording of CSs from normal and connexin36 knockout (Cx36KO) mice. The Cx36KO mouse is useful, because although there are now more than 20 identified members in the connexin family, Cx36 appears to form the overwhelming majority of neuronal gap junctions in the CNS, including the IO, and conversely, is not present in gap junctions formed between glial cells (17,18). Moreover, anatomical studies indicate normal gap junctions are absent in the IO of Cx36KO mice (19), and recordings of IO neurons in vitro from Cx36KO mice have shown that these cells lack electrical coupling (or at most are very weakly coupled relative to IO cells of Wt mice), and that the subthreshold oscillations of their membrane potentials are not synchronized, which contrasts with the case in Wts (5).

We obtained recordings from these mice to test whether CS synchrony is lost in the absence of IO neuronal electrical coupling, and whether the climbing fiber reflex, which has been attributed to electrical coupling of IO neurons, is truly dependent on this coupling. Zebrin II staining of the cerebellar cortex and anterograde tracing were also carried out in order to characterize the topographic organization of the olivocerebellar pathway in the Cx36KO mouse and to assess whether the physiological differences observed between the Cx36KO and Wt mice reflected anatomic factors other than loss of gap junction coupling of IO neurons.

Materials and methods

Experiments were carried out in accordance with the National Institutes of Health guidelines for the care and use of laboratory animals. Experimental protocols were approved by the IACUC committee of New York University School of Medicine.

Recordings were obtained from Wt and Cx36KO mice derived from the C57BL6 strain. Cx36 KOs were generated and genotyped as described previously (20).

Surgical preparation and electrode implantation

Six- to twelve-month-old mice were anesthetized with an initial intraperitoneal injection of ketamine (100 mg/kg) and xylazine (8mg/kg); supplementary doses were administered as needed starting 1–2 hours after the initial dose. A tracheal tube was inserted to allow mechanical ventilation and delivery of supplemental oxygen. Body temperature was monitored with a rectal thermometer and

maintained at $\sim 37^{\circ}$ C by means of a heating pad. The animal was placed in a stereotaxic apparatus and a ground screw was inserted into the skull over the cerebral cortex on the side contralateral to the recording area. Recordings were made of spontaneous and evoked CS activity from lobules crus 2a and 2b. To access these areas, the skin, muscle, bone and dura over the cerebellum were removed, and a platform was cemented in place over the cerebellum. The platform, an electron microscope grid encased in silicone rubber and fixed to tungsten rods, guided electrode placement and served to hold the electrodes in place after their release from the manipulator. Glass microelectrodes ($\sim 2 \mu\text{m}$ tip; 1:1 NaCl:glycerol) were individually attached to a joystick-controlled 3-axis micromanipulator (Marzhauser, Germany) by a wax droplet and inserted through the grid. When CS activity was isolated in the molecular layer, approximately $50 \mu\text{m}$ below the cortical surface, the wax was melted in order to release the electrode, which was thereafter held in place by the silicon rubber. Electrodes were spaced $\sim 250 \mu\text{m}$ apart to form arrays of up to 9 rostrocaudal columns and 3 mediolateral rows.

Recording of spontaneous CS activity

CSs were recorded using a multichannel amplifier system (MultiChannel Systems, Germany), which consisted of 128 amplifier channels (total gain 1000x) with bandpass filters of 0.1 Hz–8 kHz, and a per channel sampling rate of 25 kHz. The electrical signals were digitally high pass filtered using a cutoff frequency of 200 Hz using MultiChannel Systems MCRack data acquisition software. A voltage threshold (individually set for each channel) was used to detect CSs. Thresholds were set so as to detect the initial deflection of the CS, which was treated as a single event. On detection of a threshold crossing, the system recorded the time and waveform of the voltage record, which were then used for subsequent off-line spike sorting and data analysis.

The MCRack software had oscilloscope and spike event displays for monitoring activity. The latter display comprised a grid onto which was mapped the electrode array such that each box in the grid corresponded to the relative location of an electrode in the brain. Each box flashed when the voltage threshold in its corresponding channel was crossed, and thus allowed for simultaneous monitoring of spike activity from the entire array. Recordings of spontaneous activity were typically made for 20–40 min periods.

Data analysis

All analyses were performed using procedures custom-written by one of the authors (EJL) for use

with IGOR analysis software (WaveMetrics, OR). Statistical significance was assessed using 2-sided Student's paired *t*-tests, and mean values are presented with their corresponding SE, unless otherwise indicated.

To measure the relationship of activity in two different cells, a cross-correlation function was calculated as follows. The spike train of a cell was represented by $X(i)$, where i represents the time step ($i=1, 2, \dots, N$). $X(i)=1$ if the CS onset occurs in the i time bin, otherwise $X(i)=0$. $Y(i)$ was the same

$$C(t) = \frac{\sum_{i=1}^N \{V(i)W(i-t)\}}{\sqrt{\sum_{i=1}^N V(i)^2 \sum_{i=1}^N W(i)^2}}$$

$$V(i) = X(i) - \sum_{i=1}^N X(i)/N, W(i) = Y(i) - \sum_{i=1}^N Y(i)/N$$

as $X(i)$, but for the reference cell. The cross-correlation coefficient, $C(t)$, was then calculated as: where $V(i)$ and $W(i)$ are the normalized forms of $X(i)$ and $Y(i)$, respectively.

A 1 ms time step was used, and thus for two spikes to be considered synchronous, their onsets must occur in the same 1 ms bin. The zero-time cross-correlation coefficient, $C(0)$, was defined as the degree of synchrony between two cells.

To assess CS rhythmicity, normalized autocorrelograms were computed for individual cells using the above formula for $C(t)$, with X and Y both representing the same spike train. A 5 ms time step was used. Thus, the autocorrelogram values could range between 1 and -1 , with the central peak always equal to 1. These individual cell autocorrelograms were averaged to obtain population autocorrelograms.

To assess the statistical significance of the experimentally observed synchrony, new 'data sets' were generated by randomly shuffling the interspike intervals of the real spike train of each cell in an experiment. For each experiment, ten such sets of shuffled spike trains were made for each cell, and $C(t)$ was determined for all pairs in a set.

Climbing fiber reflex experiments

The cerebellum was exposed, as described above; however, instead of the recording platform, Gelfoam soaked in Ringer's solutions was used to cover the cerebellar surface. A bipolar stimulating electrode was inserted into the cerebellar white matter in the lobule rostral to the desired recording area. Single shocks (100 μ s, 150–600 μ A pulses) were delivered every 2 s and evoked responses were recorded with a single microelectrode. Electrical signals were fed into one channel of the multichannel amplifier described earlier.

Zebrin staining

Cx36KO and Wt mice were anesthetized with Nembutal (75 mg/kg i.p.) and perfused transcardially with phosphate-buffered saline (PBS; pH 7.4) and 4% paraformaldehyde in 0.1 M PB. Whole brains were removed and post-fixed in perfusate for an additional 2 h and subsequently rinsed and stored overnight at 4°C in 0.1 M PB, pH 7.4, containing 10% sucrose. The brainstem and cerebellum were embedded in 10% gelatin and 10% sucrose. Tissues were fixed in 10% formaldehyde and 30% sucrose solution at room temperature for 2 hours. Serial sections of 40 μ m were cut on a cryo-modified sliding microtome (Leica SM2000R) and collected in vials containing 0.1 M PB. The vials were rinsed in PBS and incubated, free floating, for 48 h in anti-Zebrin II (1:150, kindly provided by Dr. R. Hawkes, Calgary, Canada) containing 2% NHS and 0.5% Triton in PBS at 4°C. After rinsing in PBS, sections were incubated for 2 h in rabbit anti mouse HRP (1:150, p260 Dako) in PBS, containing 2% NHS and 0.5% Triton. Subsequently, sections were thoroughly rinsed in 0.05 M PB and incubated in a DAB staining for 15–20 min and rinsed in 0.05 M PB. All sections were mounted on slides in a chromic alum solution, air-dried, and counterstained with thionin. Subsequently, slides were dehydrated in graded alcohol and xylene and coverslipped with Permount.

Intraolivary BDA-injections

Cx36KO and Wt mice were anesthetized with a ketamine/xylazine mixture (65 mg/kg and 10 mg/kg, respectively) administered intraperitoneally. The body temperature was monitored and kept at $\sim 37^\circ\text{C}$ using a heating pad. After surgery, the ventral surface of the medulla oblongata was exposed for exploration of the IO. Subsequently a recording pipette was filled with 10% BDA-10,000 MW (Molecular Probes, Leiden, The Netherlands), positioned in the IO and multiple iontophoretic injections were made using a constant positive current (8 μ A; 7 seconds on/off cycle for 10 min). After 5–7 days the mice were deeply anesthetized with Nembutal (75 mg/kg i.p.) and perfused transcardially with phosphate-buffered saline (PBS; pH 7.4) and 4% paraformaldehyde in 0.1 M PB. Brains were removed and post-fixed in perfusate for an additional 1 h and subsequently rinsed and stored overnight at 4°C in 0.1 M PB, pH 7.4, containing 10% sucrose. The brainstem and cerebellum were embedded in 10% gelatin and 10% sucrose. Tissues were fixed in 10% formaldehyde and 30% sucrose solution at room temperature for 2 h. Serial sections of 40 μ m were cut on a cryo-modified sliding microtome (Leica SM2000R) and collected in vials containing 0.1 M PB. Sections containing the BDA injection sites were incubated overnight at 4°C in avidin-biotin-peroxidase complex (Vector

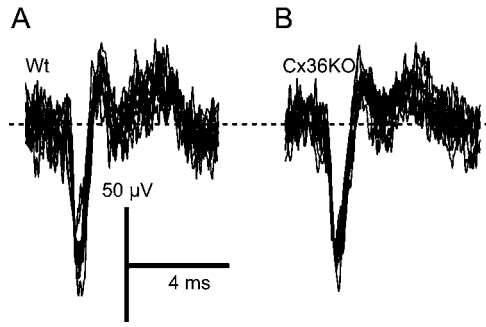


Figure 1. Complex spikes have similar waveforms in Wts and Cx36KOs. (A,B) Extracellular recording of CSs from crus 2a in a Wt (A) and Cx36KO (B) mouse. In each panel 10 overlapped traces are shown. Note the typical waveform in both cases: a large initial negativity followed by smaller wavelets riding on a slow positivity.

Laboratories, Inc., Burlingame, CA), rinsed again, and finally incubated in DAB (75 mg/100 ml) and 0.02% Cobalt chloride. The reaction was stopped after 15 min by rinsing in PB. In order to identify the climbing fibers within their zonal projections, a Zebrin staining protocol was applied as above.

Results

CS synchrony is reduced in Cx36KOs compared to Wts

Extracellular CSs were recorded from groups of crus 2 Purkinje cells in Wts ($n=9$ animals, 105 cells,

484 cell pairs) and in Cx36KOs ($n=6$ animals, 37 cells, 112 cell pairs). CS activity was recorded from both Wt and Cx36KO mice at depths of $\sim 50 \mu\text{m}$ from the folial surface, and typically consisted of a high frequency burst with a large initial negative-going deflection followed by 2–3 smaller spikes riding on a slow positivity (Figure 1).

The role of Cx36 gap junctions in mediating CS synchrony patterns was assessed using multiple electrode arrays to record CSs from groups of Purkinje cells in Wts and Cx36KOs. Typical results for a Wt and Cx36KO are shown in figure 2A1, in which the synchrony distribution relative to a master reference cell ‘M’ is presented in each bubble graph. Here, each circle shows the position of a recorded cell relative to cell M, and its area corresponds to the degree of synchrony between the cell at that location and cell M. In the Wt, cell M’s activity is more strongly synchronized with the activity of its neighbors (0–250 μm) than with the activity of cells at greater mediolateral distances from it, consistent with previous findings in other species (21). The rapid reduction in synchrony with mediolateral distance combined with a much lesser decrease with distance in the rostrocaudal direction leads to a rostrocaudal banding pattern, such as demonstrated by the Wt bubble graph of Figure 2A1. Although the sharpness of the banding pattern varies with choice

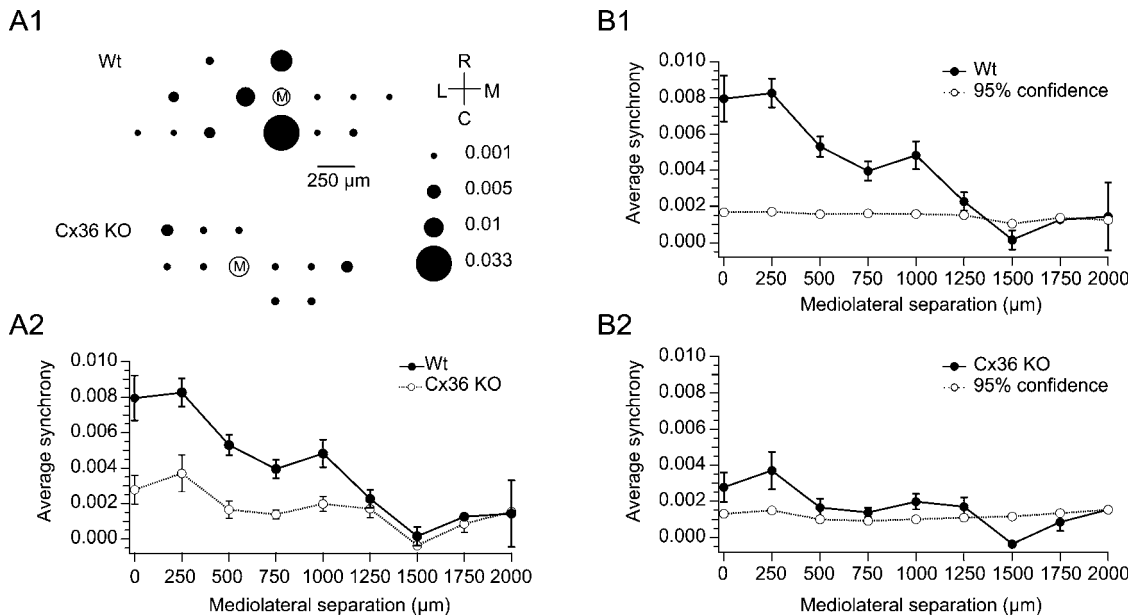


Figure 2. Comparison of CS synchrony distribution in the Wt and Cx36KO. (A1) Bubble plots show the relative positions of electrodes in the recording array from one Wt and one Cx36KO experiment. The area of each bubble corresponds to the degree of synchrony between that cell and the reference cell (labeled ‘M’). Note the high synchrony surrounding cell M in the Wt but not in the Cx36KO. (A2) Graph of average CS synchrony values between all cell pairs plotted as a function of mediolateral separation between cells for Wts (filled circles) and Cx36KOs (open circles). All cell pairs from 9 animals (Wt) and 6 animals (Cx36KO) were used to calculate averages. Error bars are SE. The number of cell pairs at each separation is as follows: for Wts, 0 $\mu\text{m}=59$; 250 $\mu\text{m}=154$ pairs; 500 $\mu\text{m}=120$ pairs; 750 $\mu\text{m}=83$ pairs; 1000 $\mu\text{m}=41$ pairs; 1250 $\mu\text{m}=20$ pairs; 1500 $\mu\text{m}=4$ pairs; 1750 $\mu\text{m}=1$ pair; 2000 $\mu\text{m}=2$ pairs; for Cx36KOs, 0 $\mu\text{m}, n=12$ pairs; 250 $\mu\text{m}, n=42$ pairs; 500 $\mu\text{m}, n=26$ pairs; 750 $\mu\text{m}, n=16$ pairs; 1000 $\mu\text{m}, n=8$ pairs; 1250 $\mu\text{m}, n=4$ pairs; 1500 $\mu\text{m}, n=1$ pair; 1750 $\mu\text{m}, n=2$ pair; 2000 $\mu\text{m}, n=1$ pair. (B) Comparison of synchrony levels in Wts (B1) and Cx36KOs (B2) to synchrony levels calculated from pairs of randomized spike trains. Synchrony curves for Wt and Cx36KO spike trains are replotted in B1 and B2, respectively. Synchrony values (95th percentile) from the randomized data values are plotted with open circles and dotted lines.

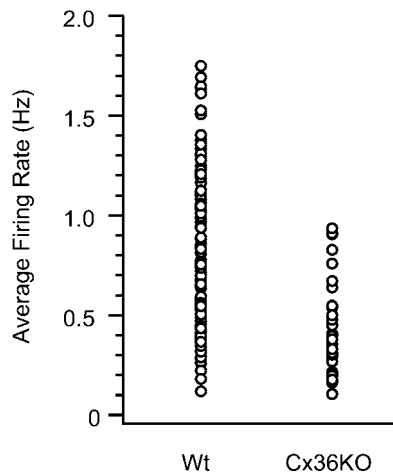


Figure 3. Cx36KOs display lower CS firing rates than Wts. CS average firing rate distributions for the Wt and Cx36KO cells. Each marker shows the value for one cell.

of reference cell, plots of average synchrony as a function mediolateral separation between cells show that these bands are the dominant pattern (Figure 2A2, filled circles). That is, ML synchrony curves in Wts were highest at small separation distances and dropped for larger separations. Note that the Wt curve in Figure 2A2 was generated from all recorded cell pairs from all Wt experiments ($n=9$ animals, 105 cells, 484 pairs).

In contrast to the Wt, a rostrocaudal banding pattern was not found in Cx36KO mice. Indeed, as shown by the example in figure 2A1, Cx36KO mice had much lower levels of CS synchrony compared to Wt animals. This reduced level of CS synchrony was confirmed by generating a mediolateral synchrony curve using all of the Cx36KO cell pairs from 6 experiments (37 cells, 112 pairs). Comparison of their mediolateral synchrony curves shows that there was significantly less CS synchrony in Cx36KOs than in Wts (Figure 2A2, open circles versus closed circles).

This difference, however, does not necessarily imply that the Cx36KOs have no statistically significant synchronization of CS activity. Indeed, while the absolute levels are low, they are above zero. On the other hand, because our data sets are finite, some degree of correlation arises because of the periodicity of CS activity. To determine the statistical significance of the CS synchrony levels in the Cx36KOs, each cell's spike train was converted to a series of interspike intervals (ISIs) that were randomly shuffled and reassembled to form a randomized spike train with the same set of primary ISIs. Ten such randomized datasets were generated from each experiment. These datasets were used to calculate synchrony values between cells. The synchrony values from all datasets of the same experimental type (i.e., Wt or Cx36KO) were combined and grouped according to mediolateral separation between cells. Both distributions

had means that were not statistically different from zero (Wt, $1.8 \times 10^{-6} \pm 1.1 \times 10^{-5}$, $n=5750$ pairs; Cx36KO, $6.7 \times 10^{-5} \pm 2.0 \times 10^{-5}$, $n=1120$ pairs). The 95th percentile value for each separation distance is plotted for the randomized Wt and Cx36KO data pairs in figures 2B1 and 2B2, respectively, which for comparison also replot the true data curves from panel A2 (filled circles). For the Cx36KO, the randomized and CS data curves are similar in value, whereas for the Wts, the CS data curve is significantly above the randomized curve. In addition, note that in both cases the randomized curves are flat in comparison to the Wt data curve, which decreases with distance.

Wt and Cx36KO mice show rhythmic ~10 Hz CS activity but have a lower average firing rate

To investigate the dependence of IO excitability and CS rhythmicity on coupling between IO neurons, we compared the firing rates and autocorrelogram characteristics of Wt and Cx36KO CSs. The average CS firing rate in the Cx36KO (0.41 ± 0.04 Hz) was half that observed in the Wt (0.82 ± 0.04 Hz; $p=2.5 \times 10^{-12}$). Additionally, the Wt firing rates had a broader range than the Cx36KO (Wt: 0.12–1.75 Hz; Cx36KO: 0.10–0.94 Hz; Figure 3).

Autocorrelograms of Wt and Cx36KO CSs revealed that in 6/8 Wt experiments and 4/6 Cx36KO experiments, rhythmic CS activity was present (Figure 4). The level of rhythmicity varied somewhat between experiments for both Wt and Cx36KOs, as shown by the examples in Figure 4; however, the strongest rhythmicity was observed in Cx36KOs (compare Figure 4A2 and 4B2). Wt oscillation frequencies had a slightly lower range than that of the Cx36KO (Wt: 6.57–10.26 Hz; Cx36KO: 8.16–14.80 Hz), but the mean oscillation frequency for Wts and Cx36KOs were not statistically different (Wt, 9.19 ± 0.50 ; Cx36KO, 9.77 ± 0.71 ; $p=0.51$).

The climbing fiber reflex is mediated by olivary gap junctions

Stimulation of the cerebellar white matter elicits two CS responses in PCs: a short latency, direct response due to direct activation of the climbing fiber, and a longer latency, reflex response that is due to antidromic invasion of the IO (22). Following demonstration of electrical coupling between IO neurons, this longer latency response has been presumed to be generated by current flow through gap junctions (3). The Cx36KO provides an opportunity to test this proposed mechanism because electrical coupling between IO neurons is nearly absent in these mice (5).

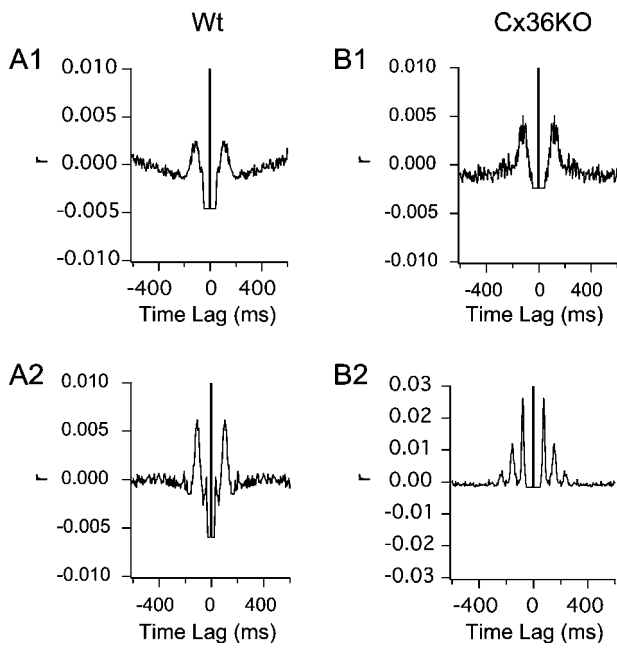


Figure 4. Rhythmic CS activity in Wt and Cx36KO mice. Normalized population autocorrelograms of CS activity from two Wt mice (A1: $n=8$ cells; A2: $n=13$ cells) and two Cx36KO mice (B1, 2: $n=5$ cells each). Peaks in the autocorrelograms indicate the presence of ~ 10 Hz rhythmic CS activity in both the Wt and Cx36KO.

Thus, responses evoked in Wt and Cx36KOs by cerebellar white matter stimulation were compared. In Wts, stimulation often evoked both direct (filled triangle) and reflex (open triangle) responses (Figure 5A1). In contrast, in Cx36KOs only direct responses could be elicited (Figure 5A2), with a

single exception. To verify that the absence of reflex responses in the Cx36KOs did not represent a sampling artifact, the spatial extent and overlap of the stimulus evoked responses in crus 2 were determined. Figure 5B compares the response distributions in a Wt and Cx36KO mouse to a similarly placed stimulation electrode (indicated by 'X'). In the Wt, direct and reflex responses both occurred in a region starting at the parasagittal plane of the stimulus electrode and extending lateral for $\sim 600 \mu\text{m}$ (Figure 5B1, B2). In the Cx36KO, direct responses were elicited from similar sites to those in the Wt (Figure 5C1), but no reflex responses were observed (Figure 5C2).

In different experiments the placement of the stimulus electrode was varied so as to test the response distribution across crus 2. In Wts, the reflex response distribution reflected the position of the stimulus electrode (Figure 6A, B). In the Cx36KOs, only one reflex response was detected (Figure 6C, indicated by '*') despite testing cortical areas that corresponded to those tested in Wts.

In total, Wts showed reflex responses in 56% of cells ($n=35/62$ cells, 10 animals), whereas in Cx36KOs only 3% of cells ($n=1/36$ cells, 3 animals) showed a reflex response. In Wt mice, reflex responses were present with (30 cells) or without (5 cells) direct responses. Moreover, of the 31 cells that had direct responses, 30 (97%) had reflex responses. In contrast, in the Cx36KO mice, 12 cells

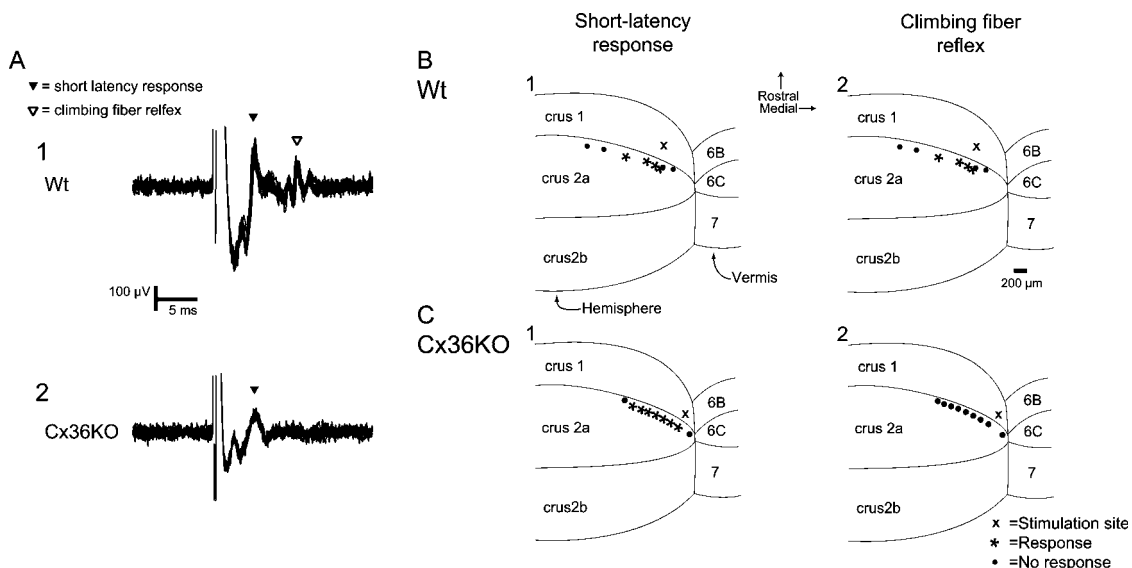


Figure 5. CF reflex responses in Wt and Cx36KO mice. (A) Extracellular traces of evoked responses to cerebellar white matter stimulation. In the Wt (A1), cerebellar white matter stimulation elicits a reflex response at ~ 10 ms (open arrowhead), which is mediated by electrotonically coupled IO neurons; this response is absent in the Cx36KO (A2). In contrast, both populations exhibit short-latency responses (A1 and 2, filled arrowhead), which are mediated by climbing fiber collaterals and are independent of IO coupling. Ten overlapped traces each. (B,C) Comparison of short latency and CF reflex distributions in the Wt and Cx36KO. In the Wt, short-latency (B1) and CF reflex responses (B2) co-occur in a limited area predominantly lateral to the stimulation site. A similar pattern of short-latency responses is observed in the Cx36KO (C1), but the CF reflex response is absent in this animal (C2). *Left column:* * = short-latency response; l = no short-latency response. *Right column:* * = CF reflex response; l = no CF reflex response.

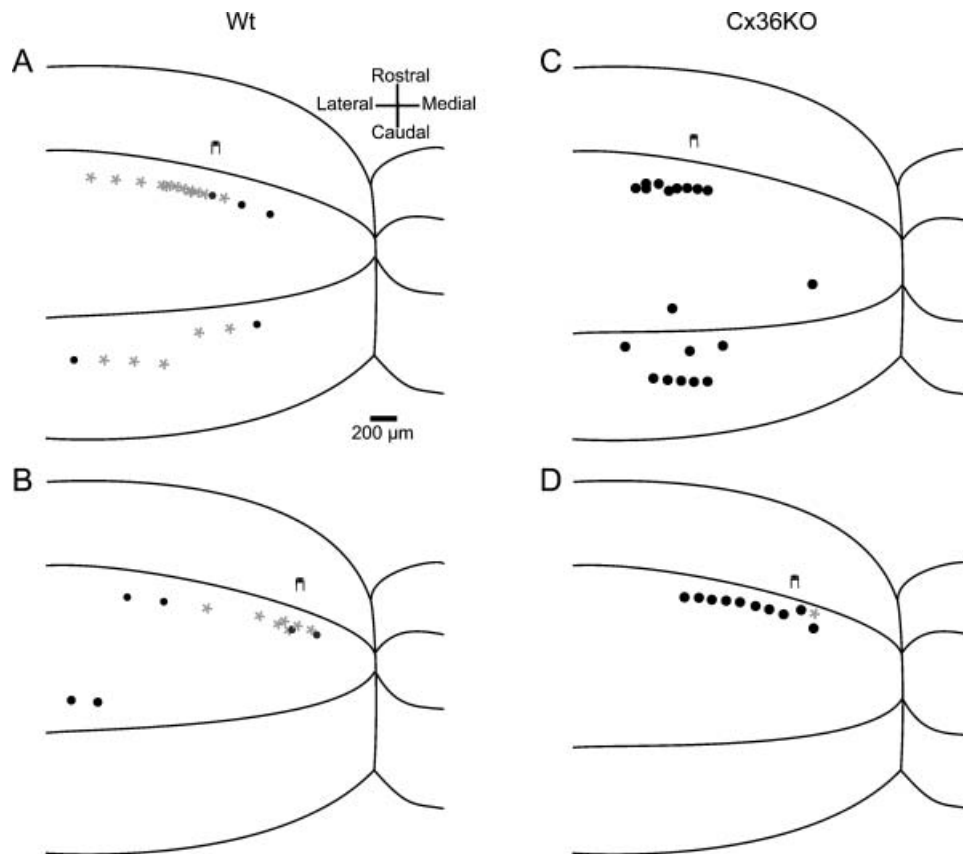


Figure 6. CF reflex response distribution in the mouse. (A,B) CS responses to white matter stimulation in Wt mice are distributed within a parasagittal band positioned slightly lateral to the stimulation site. (A) Distribution of recording sites in crus 2a and b from 3 Wts in which the stimulation electrode (n) was placed at the same location, near the middle of crus 1. An asterisk indicates that CF reflex and short-latency responses were elicited at that recording site. l=no response. (B) Same as A, except that recordings were from 3 additional animals in which the stimulation electrode was placed more medially on crus 1. (C) Distribution of recording sites in crus 2a and b from two Cx36KOs in which the stimulation electrode was placed near the middle of crus 1. λ=short-latency responses only. (D) Same as C, except responses obtained for cells from two additional animals in which the stimulus electrode was placed more medially on crus 1. One cell showed both short latency and reflex responses (indicated by the asterisk).

showed direct responses, but only one cell showed a reflex response (8%).

Zonal organization is not affected by elimination of gap junctions

The cerebellar cortex is divided into different cortical zones defined by olivo-cortico-nuclear-connections. This zonal organization can be determined by specific biochemical markers that correlate the organization of cortical zones to their distribution in the cerebellar cortex. One of these markers, Zebrin II (Aldolase C), is confined to a specific subset of Purkinje cells, resulting in a parasagittal pattern in the cerebellar cortex. Immunolabeling against Zebrin II provides a highly reproducible and consistent staining. Thus, we compared this labeling pattern in Wt ($n=2$) and Cx36KO ($n=2$) mice to determine whether absence of gap junctions would affect this zonal organization. In Wt cerebellum, immunolabeling showed a distinctive strip-like pattern with labeled and non-labeled areas, which are called P+ and P- respectively. Labeling was

restricted to the cerebellar cortex (Figure 7A). The same general labeling pattern was found in Cx36KO cerebellum (Figure 7B). Moreover, the distribution of parasagittal bands in the cerebellar cortex of the Cx36KO was identical to that in Wt. This similarity was confirmed for both vermal and hemispheric portions of all cerebellar lobules. This similarity in zebrin-positive and negative bands indicates that the zonal compartmentation is not affected in Cx36KO mice.

Because the organization of cortical zones in Cx36KO and Wt mice are equivalent, climbing fiber projections can be compared with the use of anterograde tracers such as BDA. Intra-olivary BDA injections were made in Wt ($n=3$) and Cx36KO ($n=2$) animals. One injection was made per animal, and the specific injection sites are superimposed on the schematics shown in Figure 8A1–2. The extent of each injection is shown by one set of colored circles. Intra-olivary BDA injections result in labeling of contralateral climbing fibers which project to a specific area within the cerebellar cortex (Figures 8A and B). Groups of

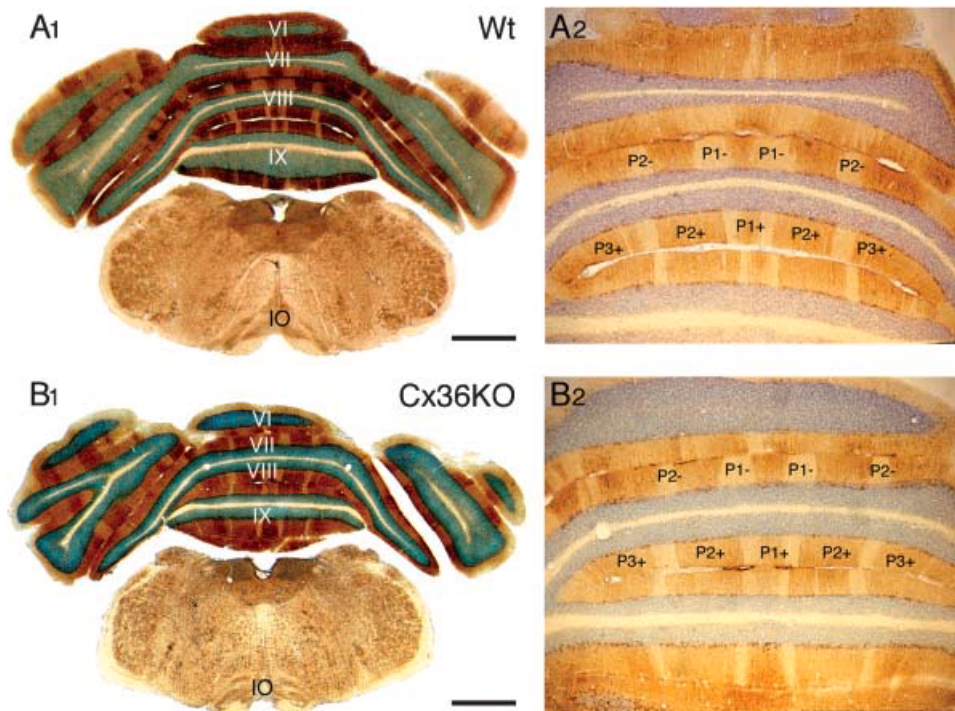


Figure 7. Cerebellar zonation patterns as revealed by zebrin II staining of Purkinje cells are indistinguishable among Wt and Cx36KO mice. (A) Zebrin stained Purkinje cell zones in a Wt mouse. (A1) Coronal section showing the brainstem and the posterior lobe (vermis and hemispheres) of the cerebellum. Lobules 6 to 9 are indicated by VI-IX. (A2) Higher magnification view of vermis portion. Zebrin II positive (P+) and negative (P-) zones are indicated. P1+ corresponds to the midline area. (B) Overview of zebrin stained Purkinje cell zones in the posterior lobe and hemispheres of a Cx36KO. Similar levels of cerebellar cortex as were shown for Wt in A. The similarity in labeling pattern to that of the Wt indicates that the zonal organization of the cerebellar Purkinje cells is not affected by a lack of Cx36 in the IO. Scale bars indicate 500 μm ; IO indicates inferior olive.

labeled climbing fibers arising from the same local IO region remain confined to essentially the same zebrin areas in Wt (Figure 8B) and Cx36KO (Figure 8C) mice. This finding suggests that climbing fiber projections in Cx36KO mice appear to have the same zonal organization as in Wt mice. Therefore, it can be concluded that Cx36KO mice show no obvious anatomical differences compared with Wt mice. Any physiological differences are thus likely the direct result of absent electrical coupling among IO neurons, rather than structural alterations within the olivocerebellar circuit.

Discussion

The present study used a Cx36KO mouse model to investigate the importance of IO gap junctions for the anatomical and physiological organization of the olivocerebellar system. The results indicate that Cx36KOs have a topographically normal olivocerebellar projection and a normal cerebellar cortical organization, but that the activity of this system is significantly altered by the loss of electrical coupling between IO neurons. In the Cx36KO, CS synchrony, which was observed in the Wt, was absent; average CS firing rates were reduced; and rhythmic CS activity was present. Lastly, the climbing fiber reflex was absent in the Cx36KOs. The implications of these findings are discussed below.

Electrical coupling of IO neurons underlies CS synchrony

Synchronous CS activity has been demonstrated in several species, including rat, guinea pig, and rabbit (6,8,21,23). The present findings extend this list to include mice. In each case, CS synchrony levels are highest among Purkinje cells located within the same parasagittally-oriented, 250–500 μm -wide strip of cortex. These strips are not limited to the folial apex, but can extend down the folial wall (24). This spatial distribution, in part, reflects the fact that the neurons of each small region of the IO project to a specific longitudinally oriented strip of cerebellar cortex (25). It also reflects the uniform conduction time of the olivocerebellar system to essentially all parts of the cortex as a result of differential myelination of olivary axons (24,26–28). There is, however, a large dynamic component to this distribution, as dramatic changes in the synchrony distribution result from blocking synaptic input to the IO (13–15), and synchrony distribution changes are also associated with voluntary movement (9).

The mechanism by which activity of olivary neurons is synchronized is the fundamental issue addressed in the present study. Ultrastructural studies indicate that the IO contains one of the richest neuronal gap junction networks in the adult CNS (2,29). Electrical coupling of IO neurons has also been demonstrated (3,11). Moreover, olivary

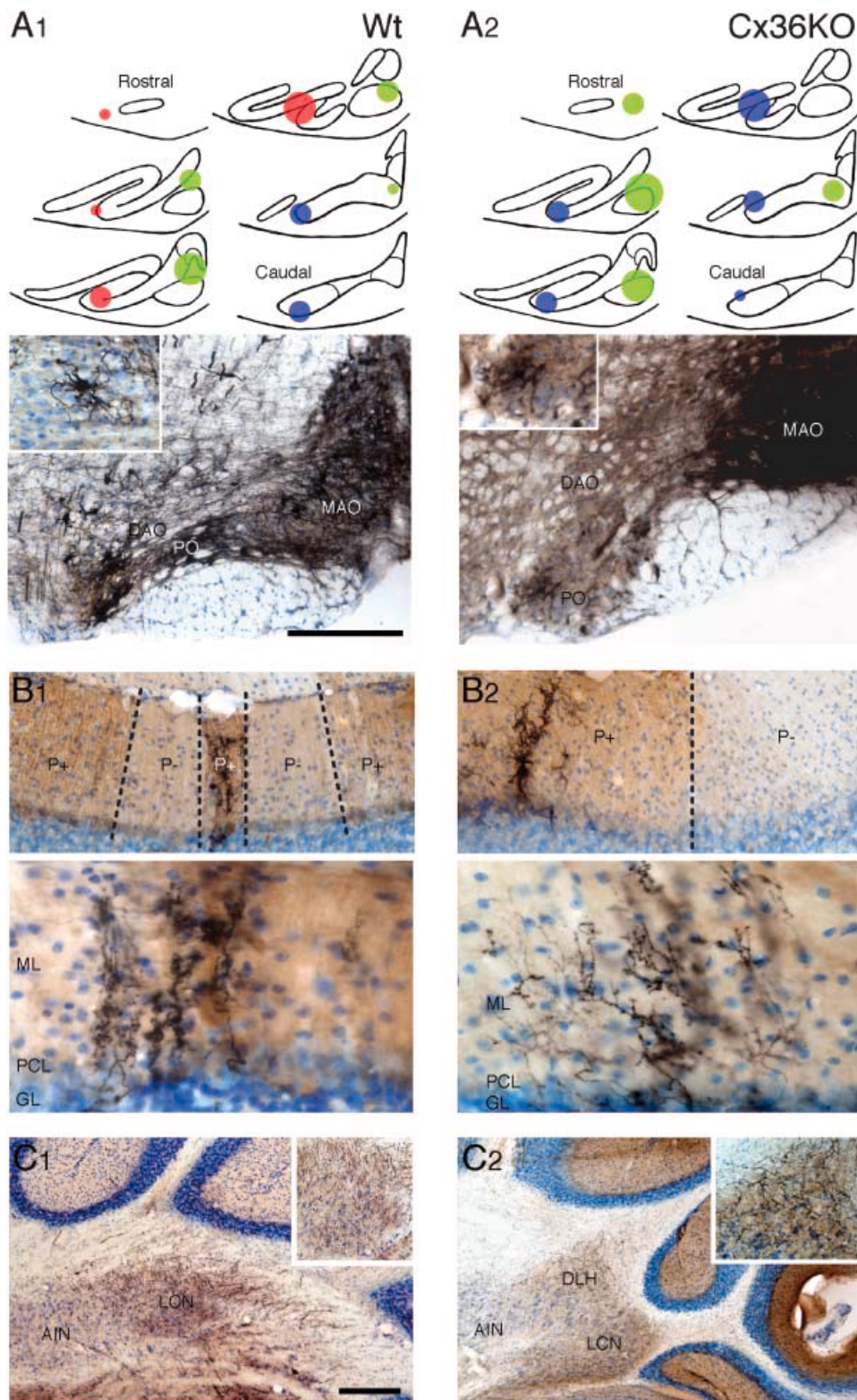


Figure 8. Cerebellar zonation patterns as revealed by anterograde tracing of olivary climbing fibers are indistinguishable among Wt and Cx36KO mice. (A) Top panels, schematic drawings of BDA injection sites in the inferior olive in Wt mice (A1) and Cx36KO mice (A2). The diameters of the circles' areas reflect the size of the injection sites within the respective subnuclei. Each set of colored circles corresponds to one injection in one animal. Bottom panels, photographs of BDA injections in the medial accessory olive (MAO); insets show examples of individual olivary neurons that took up BDA in the areas bordering the core of the injection site. (B) Anterograde labeling of climbing fibers in Wt mice (B1) and Cx36KO mice (B2) at lower (top panels) and higher (lower panels) magnifications. In these examples the labeled climbing fibers are in both wild types and Cx36KO mice restricted to zones that are positively labeled for zebrin II. (C) Lower and higher (insets) magnifications of BDA labeled climbing fiber collaterals in the cerebellar nuclei. Abbreviations: PO, principal olive; DAO, dorsal accessory olive; AIN, anterior interposed nucleus; LCN, lateral cerebellar nucleus; DLH, dorsolateral hump (Scale bar in A1 indicates 100 μm ; scale bar in C1 indicates 20 μm).

neurons are almost all projection cells that do not have local axon collaterals (30,31). These observations leave two major choices for the cause of synchronous CS activity: electrical coupling of IO neurons by gap junctions and synchronized activity in IO afferents. The latter possibility has been mostly ruled out by studies which demonstrated the continued presence of CS synchrony following block of the major excitatory (glutamate) and inhibitory (GABA) inputs to the IO (13–15).

In contrast, the present results support the first possibility, namely that synchronous CS activity requires electrical coupling of IO neurons. Our results are consistent with previous studies that investigated this issue. For example, the density of gap junctions, as judged by the presence of lamellar bodies, in the set of IO regions that project to the flocculus was correlated with the level of CS synchrony in corresponding parts of the flocculus (32). Also, *in vitro* studies of IO neurons from Cx36KO mice showed that subthreshold oscillations in neighboring cells, which are in phase in normal animals, are not so in the knockout (5). Moreover, pharmacological block of IO gap junctions by local injections of carbenoxolone were shown to reduce or eliminate CS synchrony (16). Most recently, a lentiviral approach was used to show that disrupting Cx36 gap junctions led to a decrease in dye coupling of IO neurons (12). While objections may be raised against each of these approaches, taken together they reinforce the common conclusion that CS synchrony is a result of IO gap junction coupling.

Given the demonstration of CS synchrony in several different species by several laboratories, as noted above, the findings of an extremely low level of 'loose' CS synchrony that is inconsistent with an electrotonic coupling mechanism in mice and of no difference in synchrony levels between Wt and Cx36KO mice reported previously (33) is surprising, and is contradicted by the present findings. The findings of Kistler et al (33) are also inconsistent with *in vitro* recordings of IO neurons, which showed precise (on a millisecond timescale) correlation of spikes in neighboring IO neurons in Wt, but not Cx36KO, mice (5). The findings of Kistler et al. (2002) are even more surprising given that uniform olivocerebellar conduction times have been observed in such widely separated vertebrates as turtles and rats (24,28), because it suggests that precise timing of CS activity is a highly conserved feature of the olivocerebellar system throughout vertebrate evolution. These previous results may be explained by the fact that the recordings were obtained using only pairs of electrodes, rather than arrays (33). Given the sampling procedure used, and the narrowness of the synchrony bands, relatively few pairs would have shown significant levels of synchrony, and they may have been missed. A second possible contributing

factor is that CS synchrony levels in the mouse indeed appear to be somewhat lower than is typically found in rats. Whether this represents a true species difference or simply a difference in the state of the preparation is not clear (mice tolerated the multiple electrode recording procedures less well than do rats). In this context, it is worth noting that any damage to the cerebellar cortex will likely lead to increased cerebellar nuclear activity, which in turn would increase GABA levels in the IO and thereby cause a reduction in CS synchrony. Thus at the least, the lower overall levels make observation of synchronous CS activity with electrode pairs more difficult and require more precise alignment of electrodes for its detection.

Electrical coupling is a determinant of IO excitability and rhythmicity

The average CS spike firing rate of Cx36KOs was approximately half that of Wts, and roughly half that of the 1 Hz spontaneous rate typically reported for normal animals. This finding suggests that gap junction coupling plays a major role in setting the excitability of IO neurons, and that current flow through gap junctions is responsible for about half of the spontaneous CS activity. This suggestion is consistent with several recent findings. Acute pharmacological block of gap junctions also led to a similar reduction in spontaneous CS firing rates (16). Moreover, spontaneous CS activity, while reduced, remains following block of major excitatory and inhibitory afferents to the IO (14,15).

Our results also suggest that electrical coupling may not be necessary for oscillatory behavior, but this is an issue in which there is much conflicting data, and one which will require further study. Cx36KOs had CS activity that was at least as rhythmic as that found in Wts. This result is somewhat in contradiction to our previous result that acute pharmacological block of IO gap junctions with carbenoxolone reduced or abolished rhythmic CS activity (16). Moreover, in that study, the degree of reduction in a cell's rhythmic activity was highly correlated with the loss of synchrony it experienced (16). One possible explanation of these divergent results is that carbenoxolone blocked ionic conductances in addition to blocking gap junctions; however, this possibility is unlikely, as two different groups have reported that carbenoxolone does not affect the major membrane conductances of IO neurons, most notably their Ca^{2+} conductances (34–37). One alternative is that some compensatory changes in the IO neurons of Cx36KOs allows them to continue generating oscillatory activity, despite their lack of coupling (19).

Other, mostly *in vitro*, studies have also reached divergent conclusions on the role of gap junctions in

determining rhythmic IO activity. These studies have primarily focused on the subthreshold oscillations that IO neurons can display in slices. Modeling, developmental, and physiological studies have led investigators to suggest that subthreshold oscillations are a population phenomena requiring gap junction coupling for its expression (4), (38–40). However, consistent with our present results, *in vitro* recordings from Cx36KOs showed that IO neurons from these mice displayed subthreshold oscillations, suggesting that individual IO neurons could act as independent oscillators (41). It was suggested, however, that subthreshold oscillations occur in Cx36KO IO neurons, despite their lack of coupling, because the membrane properties of these cells are altered as a compensatory response to the mutation (19). But it is not clear that the observed changes, increased input resistance and generation of low threshold Ca^{2+} spikes during hyperpolarizing current pulses, are not simply the direct consequence of the loss of electrical coupling, rather than compensatory changes in the composition or density of membrane channels. In fact, after application of gap junction blockers normal rat IO neurons *in vitro* are still capable of generating subthreshold oscillations and of generating Ca^{2+} spikes during a hyperpolarizing current pulse (34,36). Other investigators, however, have found that subthreshold oscillations are greatly diminished by application of carbenoxolone or disruption of gap junctions using a lentiviral vector to cause expression of mutated nonfunctional connexin36 (12). In sum, while it seems clear that electrical coupling will act to constrain the oscillatory behavior of IO neurons, it is difficult to reach a definite conclusion about their absolute requirement from the above data.

Climbing fiber reflex responses are triggered by currents flowing through gap junctions

The climbing fiber reflex was first described by Eccles et al. in 1966, who reported that cerebellar white matter (juxtastigial) stimulation could elicit not only a short latency CS response due to evoked action potentials traveling a purely axonal, intracerebellar route, but also a longer latency reflex CS response. Those authors speculated that the reflex response was due to a synaptic activation of IO cells either by climbing fiber or mossy fiber collaterals (22). Subsequently, however, electrical coupling of IO cells, rather than synaptic excitation, was implicated as the most likely underlying mechanism for reflex responses by both the discovery of gap junctions between IO cells and the demonstration that juxtastigial stimulation evoked a gap junction mediated, ‘short-latency depolarization’ in IO cells, which could trigger spikes in IO cells (2,3).

The latter interpretation is also consistent with the facts that there appear to be no intra-IO collaterals

from olivocerebellar axons (30), and that reflex responses still can be elicited following intra-IO injection of glutamate and GABA receptor antagonists (14,15). Moreover, reflex responses disappear following intra-IO injection of carbenoxolone (16).

In sum, it is clear that the climbing fiber reflex does not require chemical synaptic transmission. Thus, when the stimulus evokes only a reflex response in a Purkinje cell, the reflex response must be the result of the Purkinje cell’s IO cell (i.e., the IO cell whose axon synapses onto that Purkinje cell) being excited by current flowing through gap junctions from neighboring IO cells. That is, antidromic spikes elicited in the axons of other IO cells result in a depolarization of these cells, which then spreads, via gap junctions, to non-antidromically excited cells and excites them to fire orthodromic spikes that return to the cerebellum and generate reflex responses.

However, when both short-latency and reflex responses are observed, as is often the case, an alternative mechanism may be considered for the reflex response generation. Namely, the short-latency response implies that the climbing fiber was antidromically activated, and when this spike reaches the IO cell it may produce a high-threshold Ca^{2+} spike in its dendrites that could in turn lead directly to orthodromic spikes returning to the cerebellum. That is, there is simply a reflection of the antidromic spike into an orthodromic spike within the same cell. Intracellular recording from IO cells provides some evidence against this self-excitation possibility, and for the gap junction mechanism (3). Juxtastigial stimulation was used to evoke antidromic activation of an IO cell, but at the same time a depolarizing current was injected into the cell triggering an orthodromic spike, which collided with the antidromic one. By annihilating the antidromic spike a gap junction mediated depolarization was revealed, and was shown to be able to trigger orthodromic spikes. Thus, even in antidromically invaded IO cells, the reflex response can be driven via gap junction mediated excitation.

Nevertheless, the above results do not rule out the possibility that the antidromic spike could trigger reflex responses if allowed to backpropagate into the soma and dendrites. The present results, however, strongly indicate that this possibility occurs rarely, if at all. That is, in the Cx36KOs the short-latency response was found in many cells, but the reflex response was, with one exception, never found. Because electrical coupling among IO neurons is not completely absent in the Cx36KO (5), this sole exception still likely represents excitation via gap junctions; however, the backpropagation mechanism may also be an explanation. Nevertheless, given the singularity of this exception, we conclude antidromic invasion does not normally lead to a secondary orthodromic response in IO cells from Cx36KOs.

We may extend this conclusion to normal animals by noting that IO cells in Cx36KO mice appear to have the same membrane conductances as normal IO cells or may in fact be somewhat more excitable than normal because of their increased input resistance (5,19), and thus should have exhibited reflex responses had backpropagation been a significant underlying mechanism.

Acknowledgements

Funding was provided by the NIH/NINDS (grant no. NS37028). The work in the group of C.I.D.Z. was supported by the Dutch Organization for Medical Sciences (ZON-MW), Life Sciences (NWO-ALW), Senter (Neuro-Bsik), Prinses Beatrix Fonds, and the European Community (EEC; SENSOPAC).

References

- Bennett MVL, Zukin RS. Electrical coupling and neuronal synchronization in the mammalian brain. *Neuron*. 2004;41:495–511.
- Sotelo C, Llinás R, Baker R. Structural study of inferior olivary nucleus of the cat: morphological correlates of electrotonic coupling. *J Neurophysiol*. 1974;37(3):541–59.
- Llinás R, Baker R, Sotelo C. Electrotonic coupling between neurons in cat inferior olive. *J Neurophysiol*. 1974;37:560–71.
- Llinás R, Yarom Y. Oscillatory properties of guinea-pig inferior olivary neurones and their pharmacological modulation: an in vitro study. *J Physiol (Lond)*. 1986;376:163–82.
- Long MA, Deans MR, Paul DL, Connors BW. Rhythmicity without synchrony in the electrically uncoupled inferior olive. *J Neurosci*. 2002;22:10898–905.
- Bell CC, Kawasaki T. Relations among climbing fiber responses of nearby Purkinje cells. *J Neurophysiol*. 1972;35:155–69.
- Llinás R, Sasaki K. The functional organization of the olivocerebellar system as examined by multiple Purkinje cell recordings. *Eur J Neurosci*. 1989;1:587–602.
- Lang EJ, Sugihara I, Welsh JP, Llinás R. Patterns of spontaneous Purkinje cell complex spike activity in the awake rat. *J Neurosci*. 1999;19:2728–39.
- Welsh JP, Lang EJ, Sugihara I, Llinás R. Dynamic organization of motor control within the olivocerebellar system. *Nature*. 1995;374:453–7.
- Lang EJ, Sugihara I, Llinás R. Olivocerebellar modulation of motor cortex ability to generate vibrissal movements in rats. *J Physiol (Lond)*. 2006;571:101–20.
- Llinás R, Yarom Y. Electrophysiology of mammalian inferior olivary neurones in vitro. Different types of voltage-dependent ionic conductances. *J Physiol (Lond)*. 1981a;315:549–67.
- Placantonakis DG, Bukovsky AA, Aicher SA, Kiem H-P, Welsh JP. Continuous electrical oscillations emerge from a coupled network: A study of the inferior olive using lentiviral knockdown of connexin36. *J Neurosci*. 2006;26:5008–16.
- Lang EJ, Sugihara I, Llinás R. GABAergic modulation of complex spike activity by the cerebellar nucleoolivary pathway in rat. *J Neurophysiol*. 1996;76:255–75.
- Lang EJ. GABAergic and glutamatergic modulation of spontaneous and motor-cortex-evoked complex spike activity. *J Neurophysiol*. 2002;87:1993–2008.
- Lang EJ. Organization of olivocerebellar activity in the absence of excitatory glutamatergic input. *J Neurosci*. 2001;21:1663–75.
- Blenkinsop TA, Lang EJ. Block of inferior olive gap junctional coupling decreases Purkinje cell complex spike synchrony and rhythmicity. *J Neurosci*. 2006;26:1739–48.
- Condorelli DF, Belluardo N, Trovato-Salinaro A, Mudo G. Expression of Cx36 in mammalian neurons. *Brain Res Rev*. 2000;32:72–85.
- Rash JE, Staines WA, Yasumura T, Patel D, Furman CS, Stelmack GL, et al. Immunogold evidence that neuronal gap junctions in adult rat brain and spinal cord contain connexin-36 but not connexin-32 or connexin-43. *Proc Natl Acad Sci USA*. 2000;97:7573–8.
- De Zeeuw CI, Chorev E, Devor A, Manor Y, Van Der Giessen RS, De Jeu MT, et al. Deformation of network connectivity in the inferior olive of connexin 36-deficient mice is compensated by morphological and electrophysiological changes at the single neuron level. *J Neurosci*. 2003;23:4700–11.
- Güldenagel M, Ammermüller J, Feigenspan A, Teubner B, Degen J, Söhl G, et al. Visual transmission deficits in mice with targeted disruption of the gap junction gene connexin36. *J Neurosci*. 2001;21:6036–44.
- Sasaki K, Bower JM, Llinás R. Multiple Purkinje cell recording in rodent cerebellar cortex. *Eur J Neurosci*. 1989;1:572–86.
- Eccles JC, Llinás R, Sasaki K. The excitatory synaptic action of climbing fibers on the Purkinje cells of the cerebellum. *J Physiol (Lond)*. 1966;182:268–96.
- Wylie DR, De Zeeuw CI, Simpson JI. Temporal relations of the complex spike activity of Purkinje cell pairs in the vestibulocerebellum of rabbits. *J Neurosci*. 1995;15:2875–87.
- Sugihara I, Lang EJ, Llinás R. Uniform olivocerebellar conduction time underlies Purkinje cell complex spike synchronicity in the rat cerebellum. *J Physiol (Lond)*. 1993;470:243–71.
- Sugihara I, Marshall SP, Lang EJ. Relationship of complex spike synchrony bands and climbing fiber projection determined by reference to aldolase C compartments in crus IIa of the rat cerebellar cortex. *J Comp Neurol*. 2007, in press.
- Lang EJ, Rosenbluth J. Role of myelination in the development of a uniform olivocerebellar conduction time. *J Neurophysiol*. 2003;89:2259–70.
- Lang EJ, Llinás R, Sugihara I. Isochrony in the olivocerebellar system underlies complex spike synchrony. *J Physiol (Lond)*. 2006;573:277–9.
- Ariel M. Latencies of climbing fiber inputs to turtle cerebellar cortex. *J Neurophysiol*. 2005;93:1042–54.
- De Zeeuw CI, Holstege JC, Ruigrok TJH, Voogd J. Ultrastructural study of the GABAergic, cerebellar, and mesodiencephalic innervation of the cat medial accessory olive: Anterograde tracing combined with immunocytochemistry. *J Comp Neurol*. 1989;284:12–35.
- De Zeeuw CI, Lang EJ, Sugihara I, Ruigrok TJH, Eisenman LM, Mugnaini E, et al. Morphological correlates of bilateral synchrony in the rat cerebellar cortex. *J Neurosci*. 1996;16:3412–26.
- Fredette BJ, Adams JC, Mugnaini E. GABAergic neurons in the mammalian inferior olive and ventral medulla detected by glutamate decarboxylase immunocytochemistry. *J Comp Neurol*. 1992;321:501–14.
- De Zeeuw CI, Koekkoek SKE, Wylie DRW, Simpson JI. Association between dendritic lamellar bodies and complex spike synchrony in the olivocerebellar system. *J Neurophysiol*. 1997;77:1747–58.
- Kistler WM, De Jeu MTG, Elgersma Y, van der Giessen RS, Hensbroek R, Luo C, et al. Analysis of Cx36 knockout does not support tenet that olivary gap junctions are required for complex spike synchronization and normal motor performance. *Ann NY Acad Sci*. 2002;978:391–404.

34. Leznik E. Spatio-temporal characteristics of oscillatory patterns in the inferior olivary nucleus. New York: New York University, School of Medicine; 2004.
35. Leznik E, Llinás R. Role of gap junctions in generating and synchronizing oscillations in the inferior olivary nucleus. *Soc Neurosci Abstr.* 2003; 274.12.
36. Leznik E, Llinás R. Role of gap junctions in synchronized neuronal oscillations in the inferior olive. *J Neurophysiol.* 2005;94:2447–56.
37. Placantonakis DG, Bukovsky AA, Zeng X-H, Kiem H-P, Welsh JP. Fundamental role of inferior olive connexin 36 in muscle coherence during tremor. *Proc Natl Acad Sci USA.* 2004;101:7164–9.
38. Yarom Y. Rhythmogenesis in a hybrid system – interconnecting an olivary neuron to an analog network of coupled oscillators. *Neuroscience.* 1991;44:263–75.
39. Bleasel AF, Pettigrew AG. Development and properties of spontaneous oscillations of the membrane potential in inferior olivary neurons in the rat. *Dev Brain Res.* 1992;65:43–50.
40. Manor Y, Rinzel J, Segev I, Yarom Y. Low-amplitude oscillations in the inferior olive: A model based on electrical coupling of neurons with heterogeneous channel densities. *J Neurophysiol.* 1997;77:2736–52.
41. Long MA, Cruikshank SJ, Jutras MJ, Connors BW. Abrupt maturation of a spike-synchronizing mechanism in neocortex. *J Neurosci.* 2005;25:7309–16.